Optik 129 (2017) 217–224

Contents lists available at ScienceDirect

Optik

journal homepage: www.elsevier.de/ijleo

Original research article

Calibration of non-Common path aberration using multi-Channel phase diversity technique

Zongyang Wang[a,b,*], Jianli Wang[a], Bin Wang[a,c], Yuan Hao Wu[a]

[a] Chanchun Institute of Optics and Fine Mechanics and Physics, Chinese Academy of Sciences, Changchun, Jilin 130033, China
[b] University of Chinese Academy of Sciences, Beijing 100049, China
[c] Northeast Normal University, Changchun, Jilin 130024, China

ARTICLE INFO

Article history:
Received 11 July 2016
Received in revised form 15 October 2016
Accepted 19 October 2016

Keywords:
Multi-channel phase diversity
Non-common path aberration
Adaptive optics

ABSTRACT

This paper provides a method of using multi-channel Phase Diversity technique for online calibration of non-common path aberration of AO system. The PD technique estimate the phase aberration by collecting one or more frames images with short time of exposure at focal plane and out-of-focus plane, meanwhile reconstruct the target image. Under the working condition of closed-loop AO system, the static aberration of imaging path can be detected online by PD algorithm and transfer the wavefront aberration coefficient into the initial form of the deformable mirror, thus compensate for the static aberration of the non-common optical path. The experiment result shows that the imaging quality is improved by a large margin after calibration, the FWHM of the point source target decreased from 8.90 to 7.64; the wavefront RMS of imaging path decreased from 0.133 λ to 0.033 λ, and PV deceased from 0.79 λ to 0.17 λ, in accordance with the wavefront aberration measured by the closed-loop. This fully testified the ability of the application in optical detection of the Phase Diversity. There is no need to modify the original adaptive optical path, and it can precisely solve the system aberration in the condition of high SNR, and is one of the ideal optical detection techniques of large-diameter optical imaging system.

1. Introduction

Adaptive Optics (AO) system is able to detect and compensate an aberrated wavefront caused by the disturbance of atmospheric turbulences in real-time, by turning it into a controlling signal and applying corrections to the wavefront corrector such that the ground-based large-diameter optical telescope receives a target image close to the diffraction limit [1]. However, the non-common path of the wavefront sensor and imaging detector is affected by the alignment error, temperature, and gravity change, so the issue of non-common path static aberration cannot be avoided. The static aberration of the imaging path cannot be detected and compensated in the practical working of AO system. Also, the close control loop of the wavefront sensor and corrector can put their static aberration into the imaging path in the calibration of the aberration of the path, further infecting the quality of imaging [2,3]. So there has been a degraded performance of the AO system due to the existence of non-common path static aberration and the coupling relations given above. Regular re-calibration before running becomes a solution.

* Corresponding author at: Chanchun Institute of Optics and Fine Mechanics and Physics, Chinese Academy of Sciences, Changchun, Jilin 130033, China
E-mail address: 356177293@qq.com (Z. Wang).

http://dx.doi.org/10.1016/j.ijleo.2016.10.059
0030-4026/

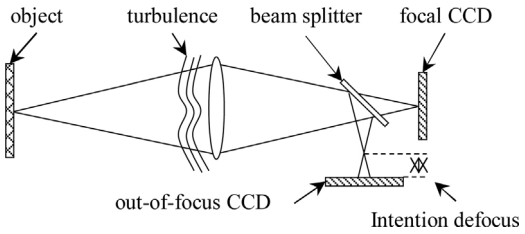

Fig. 1. Phase Diversity Principle.

Phase Diversity, also known as the PD, as an efficient way of reconstruction of the image in order to deal with wavefront aberration, developed by Gonsalves et al. PD utilizes a pair of simultaneously collected two-channel images with short time of exposure to estim,te both the system aberrations and the clear target images. Paxman et al. further improved the PD theory by working out a math model for multi-channel and multi-frame under Gauss and Poisson noises [4], which has lifted the accuracy of PD estimation under the circumstances of noise [5]. Mugnier and Blanc etc., have developed a PD Marginal Estimator theory [6,7], and applied the PD technique into the calibration of NAOS and CONICA static aberrations and of AO system. An efficient posteriori theory for identification of static aberrations of AO system was summarized through simulation and experiments [8–10]. The structure of PD optical system is simple, applies for both point source targets and random extended targets, is able to solve for dynamic atmosphere aberrations and system static aberrations. And so far the application of Phase Diversity has been expanded from reconstruction of image to the field of Optical Detection [11].

This paper introduces an online method of calibration of static non-common path aberrations of meter-level-diameter AO optical telescope using PD technique, based on the above researches. By setting up an optical fiber source at the first image plane as the observing target, we detect and compensate for the static aberration of the path from the first image plane to the wavefront sensor in real time, under the working condition of the closed loop of Shack–Hartman wavefront sensor (SH-WFS) and deformable mirror; meanwhile, we use PD algorithm to detect static aberration of imaging path online, then transfer the wavefront aberration coefficient that we get into the initial form of the deformable mirror, thus compensate for the static aberration of the non-common optical path.This paper at first introduces PD theory in detail, then gives equation evaluating for online detection. At last, the paper describes the experiment of observing star point and detection of non-common optical path static aberration on CIOMP 1.23 m caliber adaptive optical telescope.

2. Basic theory of phase diversity

Fig. 1 shows the layout of PD theory. A known defocus is added with a Beam Splitter added to the path of defocus channel. For static aberration, we can obtain the multi-channel images by the focusing mechanism. PD algorithm can be considered as a math problem which out-of-focus image is known and the target and wavefront phase is to be solved. The using of multi-channel images can effectively resolve the absence of the solutions uniqueness by adding constrains [12–16]. And the using of images with short time exposure increases signal to noise ratio of the reconstruction target [17–20].

2.1. Imaging system

The combination of atmosphere and the telescope is approximately a linear-invariant system. When illuminating with spatially incoherent light, the imaging equation of the Gauss noise model in spatial domain is as following [2]:

$$d(x) = \mathrm{o}(\mathrm{x}) * s(x) + n(x), \tag{1}$$

If not specified, lowercase letters indicate the spatial domain while uppercase letters express the frequency domain. In the above formula, d refers to the detected image on the CCD, o is the true object, s is the point spread function (PSF), n is Gauss noise, and x refers to the coordinate vector in the image plane.

Under the far-field approximation, the point spread function (PSF) can be given by the following equation [2]:

$$s(x) = |\mathcal{F}^{-1}\left\{p(\upsilon)e^{i\phi(\upsilon)}\right\}|^2, \tag{2}$$

where $\mathcal{F}^{-1}$ means the Fourier transform, υ is the coordinate vector in pupil plane, and p is the pupil function. ϕ is the wavefront phase which can be defined by a sum of Zernike polynomials:

$$\phi(\upsilon) = \theta(\upsilon) + \sum_{m=4}^{M} \alpha_m z_m(\upsilon), \tag{3}$$

where α_m and z_m is the corresponding Zernike polynomial coefficients and bases of the mth sub-mirror, respectively. θ is the known defocused phase invariable [21–23].

2.2. Valuation function

A metric for regularization can be derived using a Bayesian maximum a posteriori interpretation of the phase diversity problem. Thus the regularized cost function can be rewritten as Joint Maximum A Posteriori, also known as JMAP metric, as:

$$(\hat{o}, \hat{\alpha})_{JMAP} = arg\max_{o,\alpha} \prod_{c} Pr(d_c|o, \alpha; \gamma) Pr(o; \gamma) Pr(\alpha), \tag{4}$$

where c is the index of defocus channel and γ is the regularization parameter which limits the amplification of noise and increases the rate of convergence. Because the static aberrations in non-common path is labeled as lower-order aberrations, $Pr(\alpha)$, the probability density function regarding α, can be considered later. Assuming δ^2 is the estimated noise variance of static white Gaussian noise, the equation of JMAP can be rewritten as:

$$J(o, \alpha) = \frac{1}{N^2} \sum_{u}^{N^2} \sum_{c}^{5} \left(\frac{|D_c(u) - OS_c(u)|^2}{\sigma^2} + \frac{|O(u)|^2}{S_o(u)} \right), \tag{5}$$

where N^2 is the sum of all pixels, u is the coordinate in frequency domain, S_o is the density of object power spectrum. In the experiment of this paper, SNR of the focal plane and defocus plane was quite high, and the target point source light is close to the Dirac function, so S_o can be simplified as a constant number, with $\sigma^2/S_o = \gamma$. This paper takes the value of 10^{-5} for it.

Taking object estimation as a medium process apart from the phase estimation, we are able to obtain a cost function unrelated to the object [3]. For the cost function, the equation for object estimation is a derivation step of it, with the form of Wiener Filter, and it can efficiently be used for noise suppression [24–26].

$$J(\alpha) = \frac{1}{N^2} \sum_{u}^{N^2} \left(\sum_{c}^{5} |D_c(u)|^2 - \frac{|\sum_{c}^{5} D_c S_c^*(u)|^2}{\gamma + \sum_{c}^{5} |S_c(u)|^2} \right), \tag{6}$$

$$O = \frac{\sum_{c}^{5} D_c S_c^*}{\gamma + \sum_{c}^{5} |S_c|^2}, \tag{7}$$

In the above equation, $*$ refers to the conjugation. After the cost function defined, the PD algorithm can be described as a nonlinear optimization process of finding extreme values. This paper adopts limited memory Quasi-Newton Method [27,28] (L-BFGS-B) which applies for simple constraints of finding the optimized in large amount of variables, and compiles optimized software based on GPU server. The rate of convergence of the algorithm proved to be good after a long-term verification.

3. Calibration of non-common path aberration

During the calibration of non-common path aberration, the telescope is on the non-observing status. In Fig. 2, we set up an optical fiber source with 1 mm diameter at the first image plane as the observing target, the static aberration of the path from the first image plane to the wavefront sensor can be detected by Hartman wavefront sensor in real time, then the wavefront processer will process the wavefront information and convert it into the control signal of the deformable mirror, thus compensate for the static aberration of the optical path. During the calibration of the wavefront aberration, the close control loop of Hartman wavefront sensor and the deformable mirror will put their static aberration into the imaging path, leading the uncertainty of the static aberration of the imaging path.

The quality of image is degraded because of the combination of the original static aberration of the first image plane to the imaging path and the additional aberration caused by deformable mirror calibration loop. This can be detected precisely through PD algorithm. Because we are mainly detecting system static aberrations, so we can adopt asynchronous collection rather than synchronous collection, which is required in the PD theory. Out-of-focus images can be obtained by moving electronic controlled focusing platform for a designated distance. Defocusing length can be preset and the error in the moving can be negligible because it is of micron level. In order to increase the accuracy of the PD algorithm, this paper takes at least 5 groups of out-of-focus images as known aberrations. While adaptive systems works, imaging path can asynchronously collect the images of focal plane and defocus plane, and can figure out wavefront aberration coefficient through PD algorithm online.

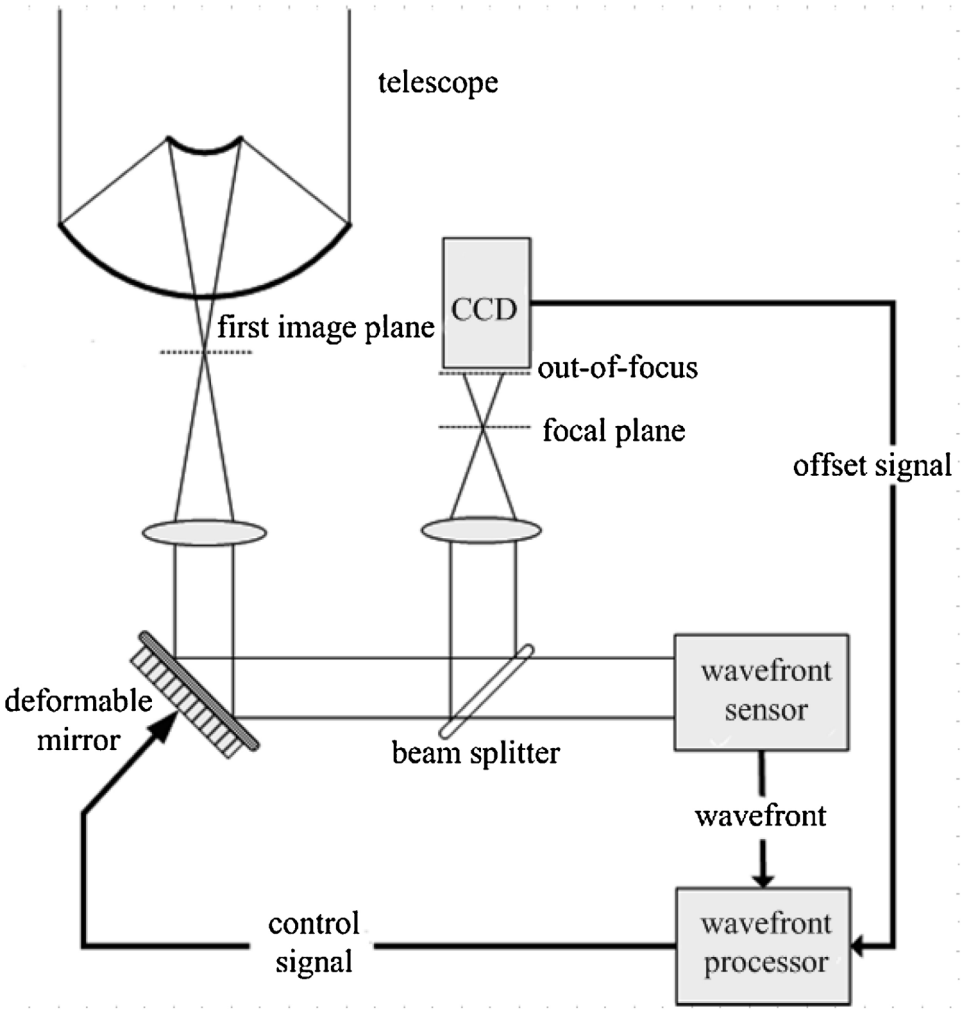

Fig. 2. Structure of AO system.

In order to further improve the calibration of the non-common path aberrations, this paper then transfer the wavefront aberration coefficient that we get into the initial form of the deformable mirror, compensating for the static aberration of the non-common optical path. And then recollect the image of focal plane and out-of-focus image, work out the system static aberration after calibration, and analyze and compare the data before and after calibration.

4. Experiments result and analysis

After Shack-Hartman wavefront sensor and the deformable mirror started to work, the wavefront phase from the first image plane to the wavefront sensor that we obtained is shown as Fig. 3b, where the RMS of the wavefront phase is 0.017 λ, PV is 0.122 λ. So the calibration of the static aberration for adaptive closed-loop path reached the requirement. But the focal plane of the imaging camera is shown as Fig. 5c, where the fiber point target becomes vague and the FWHM is 8.90. By comparing the before and after out-of-focus images, we are able to tell that there is static aberration we cannot ignore in the imaging path.

This paper selected five-channel fixed defocus aberration images for defocus length at −20 mm, −10 mm, 0 mm, 10 mm, and 20 mm to detect static aberration for imaging path using Phase Diversity. The wavefront phase is shown as Fig. 4a, where RMS is 0.13 λ and PV is 0.79 λ, higher than the data of the adaptive closed-loop path. Table 1 is a list of the 5th–13th Zernike low-order aberration coefficients before and after calibration of the static aberration. In the first column of Table 1, the coefficients of astigmatism, coma, and spherical aberration are all higher than the other values, but are all below 1/10 λ, the static aberration is difficult to be removed by exquisite alignment and adjustment.

In order to compensate for the static aberration of imaging camera path, this paper takes five of the highest value in the first column of Table 1 as the offset coefficients and feedback to the wavefront processor, and then transfer into the initial

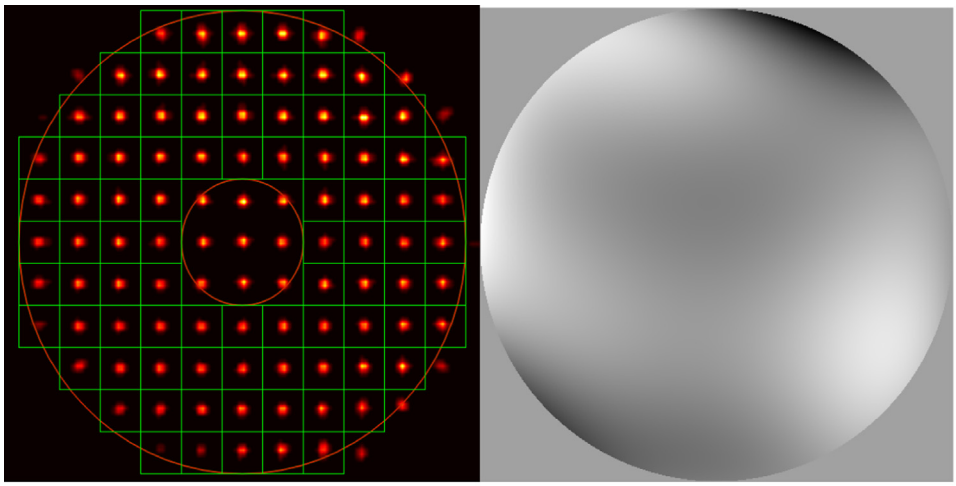

Fig. 3. Wavefront phase by Shack-Hartmann.

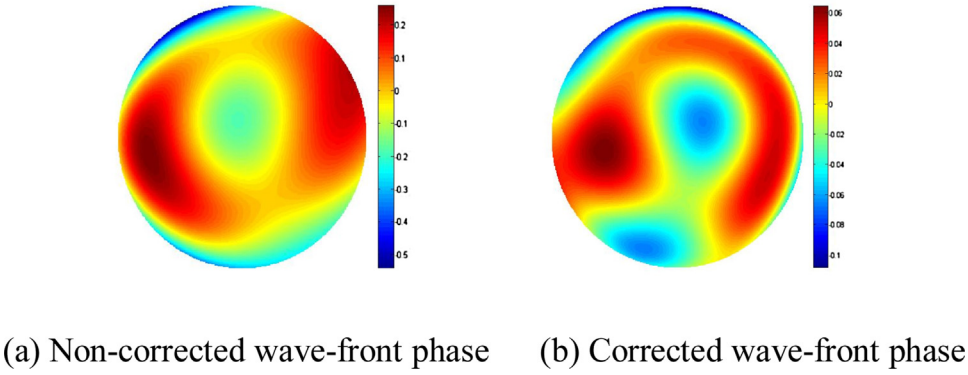

Fig. 4. Wavefront phase by PD.

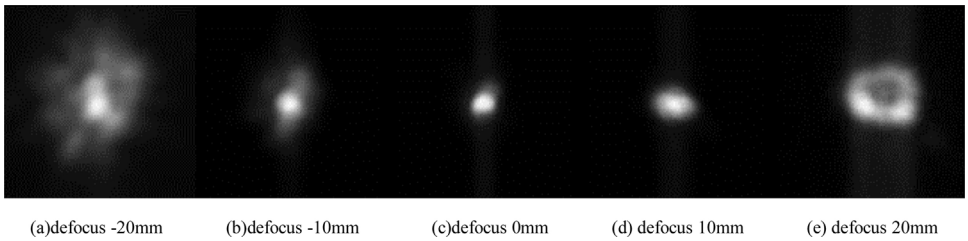

Fig. 5. Multi-channel images collected by CCD camera before calibration.

Table 1
Zernike coefficient by Phase Diversity.

Zernike Polynomials	Before Calibration	After Calibration
Astigmatism y	−0.0413	0.0001
Astigmatism x	**0.0743**	**0.0162**
Coma y	**0.0332**	**0.0027**
Coma x	−**0.0284**	**0.0105**
Trefoil y	0.0074	0.0065
Trefoil x	0.0092	−0.0081
Spherical	−**0.0745**	−**0.0182**
Secondary astigmatism y	−0.0074	−0.0038
Secondary astigmatism x	−0.0004	0.0024

The significance of bold values is minus.

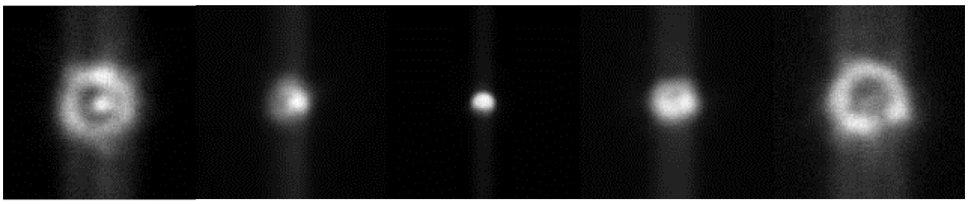

(a)defocus -20mm (b)defocus -10mm (c)defocus 0mm (d) defocus 10mm (e) defocus 20mm

Fig. 6. Multi-channel images collected by CCD camera after calibration.

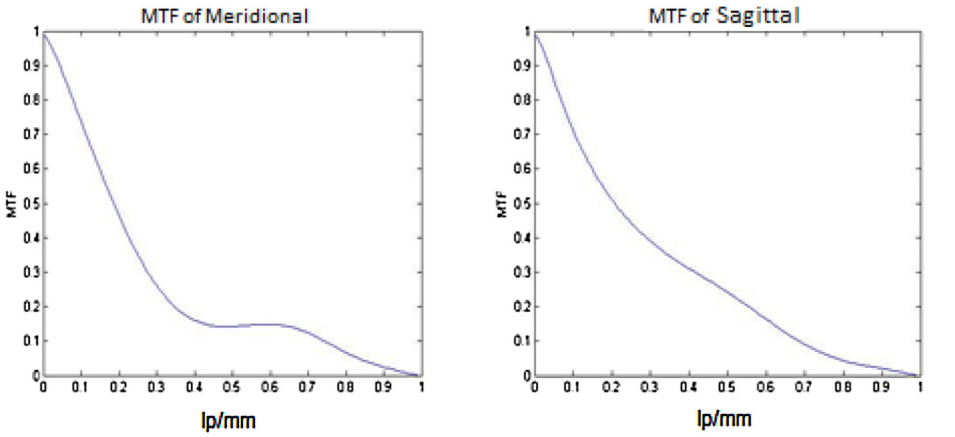

(a) MTF of Meridional before calibration (b) MTF of Sagittal before calibration

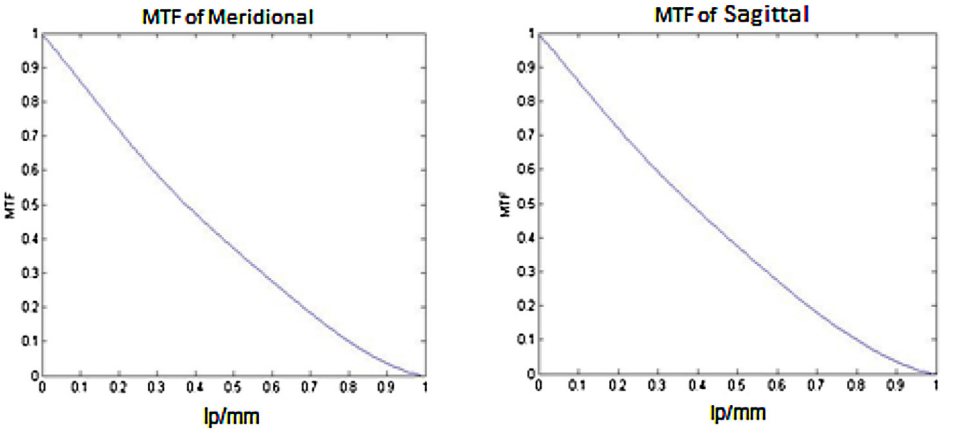

(c) MTF of Meridional after calibration (d) MTF of Sagittal after calibration

Fig. 7. Value of MTF.

form of the deformable mirror. The focal plane image of the imaging camera after calibration is shown as Fig. 6c, where FWHM decreases to 7.64. The imaging quality is improved obviously, with sharp outline of the fiber point light source. Then this paper further collect multi-channel out-of-focus images of the imaging camera after calibration, meanwhile adopt imaging path system aberration calibrated by PD algorithm, the wavefront phase is shown as Fig. 4b, where RMS decreased to 0.033 λ and PV decreased to 0.171 λ, which in accordance with the aberration measured by adaptive closed-loop path. The second column of Table 1 suggests that the five highest ones are well-suppressed, and the other coefficients haven't been changed obviously. This means that there has been a good performance of the calibration of non-common path aberration. By comparing Meridional and Sagittal curves of the Modulation Transfer Function (MTF) that solved by PD algorithm, shown as Fig. 7, we can see that the MTF curve size increases after calibration, relative slope decreases, close to the diffraction limit.

After calibration of non-common path aberration, this paper carried out Polaris observations with 1.23 m diameter telescope. For verification of the calibration, this paper recorded image data before and after adding aberration calibration

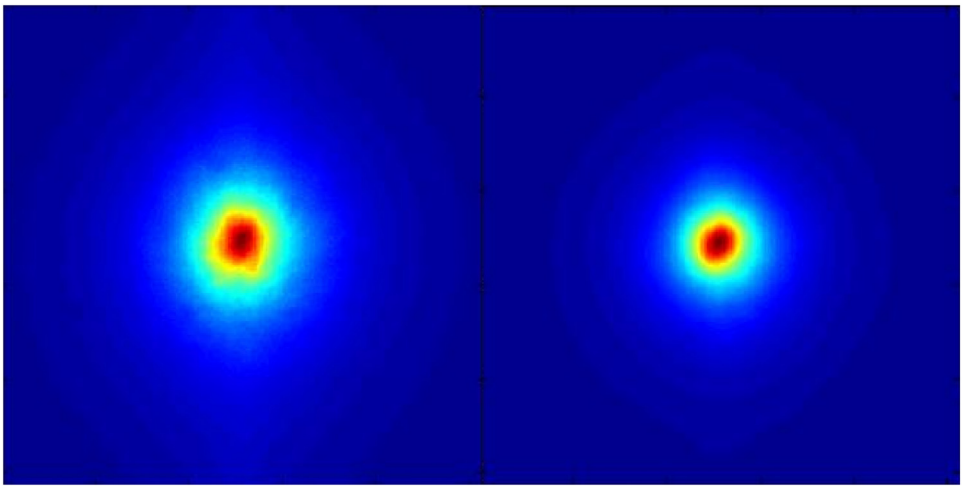

(a) before calibration (b) after calibration

Fig. 8. Polaris imaging by AO.

coefficient to the deformable mirror, worked out the average of 100 frames of continuous images for each group of data. The result shows that FWHM decreased from 13.08 to 11.52 after calibration, and the energy concentration degree improved (Fig. 8).

5. Conclusion

This paper provides a method of using multi-channel Phase Diversity technique for online calibration of non-common path aberration of AO system, increasing the imaging quality of AO system by a large margin. Under the working condition of adaptive closed-loop system, we can figure out online the original and additional non-common path aberrations using focal plane image and out-of-focus image collected by imaging path, and transfer the wavefront phase that obtained by PD algorithm into the initial form of the deformable mirror, leading to a clear target image after calibration. The experiment result shows that, after calibration of non-common path static aberration, the FWHM decreased by around 14%, system aberration decreased by 74%, and system aberration is in accordance with the aberration measured by adaptive closed-loop path. The result proved the possibility of solving wavefront phase and application in optical detection of using PD algorithm. Using this method, there is no need to modify the original AO path to obtain the out-of-focus image; focusing mechanism simply can satisfy the need. The online calibration of non-common path aberration can be conducted before each time of observation, and it is a quite ideal technique of calibration of non-common path static aberration.

References

[1] M.C. Roggemann, B.M. Welsh, Imaging Through Turbulence, CRC Press, Washington, 1996.
[2] R.G. Paxman, T.J. Schulz, J.R. Fienup, Joint estimation of object and aberrations by using phase diversity, Opt. Soc. Am. A9 (1992) 1072–1085.
[3] R.G. PAXMAN, J.H. SELDIN, M.G. Löfdahl, et al., Evaluation of phase-diversity techniques for solar-image restoration, Astrophys. J. 466 (1996) 1087–1099.
[4] M. Nizan, N.R. Erez, S. Shy, Point spread function estimation from projected speckle illumination, Light: Sci. Appl. 5 (2016) e16048.
[5] S. Adi, F. Nairouz, S. Shy, Correction-free remotely scanned two-photon in vivomouse retinal imaging, Light: Sci. Appl. 5 (2016) e1600.
[6] A. Blanc, L.M. Mugnier, L.M. Idier, Marginal estimation of aberrations and image restoration by use of phase diversity, Opt. Soc. Am. 20 (6) (2003) 1035–1046.
[7] A. Blanc, T. Fusco, M. Hartung, et al., Calibration of NAOS and CONICA static aberrations Application of the phase diversity technique, Astron. Astrophys. 399 (2003) 373–383.
[8] K.S. Pawan, T.C. Young, C. Daping, A high-resolution optically addressed spatial light modulator based on ZnO nanoparticles, Light: Sci. Appl. 4 (2015) e259.
[9] M. Hartung, A. Blanc, T. Fusco, et al., Calibration of CONICA static aberrations by phase diversity technique, Proc. SPIE 4841 (2003) 295–306.
[10] W.Q. Zhao, W.Y. Li, J.Y. Zhao, et al, Surface measurement by randomly phase shifting interferometer of measured element, Opt. Precis. Eng. 24 (9) (2016) 2167–2712.
[11] F.P. Valeriano, P. Sandy, F. Karsten, et al., Solving the inverse grating problem by white light interference Fourier scatterometry, Light: Sci. Appl. 1 (2012) e36.
[12] J.B. MARTIN, Adaptive optical microscopy: the ongoing quest for a perfect image, Light: Sci. Appl. 3 (2014) e165.
[13] W.J. Li, Q.Q. Mu, S.X. Wang, et al., High precision adjustable mechanism for Shack-Hartmann senser, Opt. Precision Eng. 23 (10) (2015) 2852–2859.
[14] P.F. Wei, X.D. Lin, M.H. Wang, et al., Simultaneous measurement of atmospheric coherence length, Opt. Precis. Eng. 24 (8) (2016) 1840–1845.
[15] X.F. Fan, W.T. Zheng, J.S. David, Light scattering and surface plasmons on small spherical particles, Light: Sci. Appl. 3 (2014) e179.
[16] Y. Zheng, J. Bian, X.L. Wang, et al., Revisiting Newton's rings with a plasmonic optical flat for high-accuracy surface inspection, Light: Sci. Appl. 5 (2016) e16156.

[17] B.J. Thelen, R.G. Paxman, D.A. Carrara, et al., Maximum a posteriori estimation of fixed aberrations, dynamic aberrations, and the object from Phase-diverse Speckle data, J. Opt. Soc. Am. A16 (1999) 1759–1768.
[18] C.R. Vogel, Computational Methods for Inverse Problems, SIAM Press, Philadelphia, 2002.
[19] C.R. Vogel, T. Chan, R. Plemmons, Fast algorithms for phase diversity-Based blind deconvolution, in: Adaptive Optical System Technologies, SPIE, Kona, Hawaii, USA, 1998, pp. 994–1005.
[20] M.G. Löfdahl, T.E. Berger, R.S. Shine, et al., Preparation of a dual wavelength sequence of high-resolution solar photospheric images using Phase Diversity, Astrophys. J. 495 (1998) 965–972.
[21] P. Maria, P. Eric, V. João, et al., Two-dimensional control of light with light on metasurfaces, Light: Sci. Appl. 5 (2016) e16070.
[22] M.R. Alexander, P.F. Michail, K.T. Sergei, The effect of self-focusing on laser space-debris cleaning, Light: Sci. Appl. 3 (2014) e159.
[23] W.J. Sun, Q. He, S.L. Sun, et al., High-efficiency surface plasmon meta-couplers: concept and microwave-regime realizations, Light: Sci. Appl. 5 (2016) e16003.
[24] M.G. Löfdahl, G.B. Scharmer, Wave-front sensing and image restoration from focused and defocused solar images, Astron. Astrophys. 107 (1994) 243–264.
[25] X.X. Ma, J.L. Wang, Surface testing with phase diversity method, Opt. Precis. Eng. 23 (4) (2015) 975–981.
[26] H.B. Liu, F.L. Chang, Moving object detection by optical flow method based on adaptive weight coefficient, Opt. Precis. Eng. 24 (2) (2016) 460–468.
[27] R.H. Byrd, P. Lu, J. Nocedal, et al., A limited memory algorithm for bound constrained optimization, in: Report NAM-08, EECS Department, Northwestern University, 1994.
[28] C. Zhu, R.H. Byrd, P. Lu, et al., LBFGS-B: Fortran subroutines for large-scale bound constrained optimization, in: Report NAM-11, EECS Department, Northwestern University, 1994, 2016.